Commun. Theor. Phys. (Beijing, China) **54** (2010) pp. 985–996

Vol. 54, No. 6, December 15, 2010

Quantum Anti-Zeno Effect in Artificial Quantum Systems*

AI Qing (艾清) and LIAO Jie-Qiao (廖洁桥)

Institute of Theoretical Physics, Chinese Academy of Sciences, Beijing 100190, China

(Received October 8, 2010)

Abstract *In this paper, we study a quantum anti-Zeno effect (QAZE) purely induced by repetitive measurements for an artificial atom interacting with a structured bath. This bath can be artificially realized with coupled resonators in one dimension and possesses photonic band structure like Bloch electron in a periodic potential. In the presence of repetitive measurements, the pure QAZE is discovered as the observable decay is not negligible even for the atomic energy level spacing outside of the energy band of the artificial bath. If there were no measurements, the decay would not happen outside of the band. In this sense, the enhanced decay is completely induced by measurements through the relaxation channels provided by the bath. Besides, we also discuss the controversial golden rule decay rates originated from the van Hove's singularities and the effects of the counter-rotating terms.*

PACS numbers: 03.65.Xp, 03.65.Yz, 85.25.Hv
Key words: quantum Zeno effect, quantum anti-Zeno effect, artificial quantum system

1 Introduction

Generally speaking, the couplings between a quantum system and a bath lead to the decay of the excitation in the system. The bath consists of many harmonic oscillators with energy spectrum over a broad band. This irreversible process requires bath's modes in approximate resonance with the system's excited level. In other words, the approximately resonant modes provide a relaxation channel for the decay of the system. Thus, this results in a nonzero decay rate in the long run according to the Fermi golden rule.[1−3]

It was found out that such spontaneous decay could be usually suppressed by frequent measurements.[4−6] This suppression phenomenon is called quantum Zeno effect (QZE). But for some cases, the above mentioned decay phenomena may be remarkably accelerated and thus the quantum anti-Zeno effect (QAZE) occurs.[7−10] In this case, the measured decay rate is larger compared with the golden rule decay rate, which is the decay rate purely resulting from the coupling to the bath in the absence of the repetitive measurements.

This enhanced decay phenomenon is generally due to the associated effects of both the coupling to the bath and the measurements. It depends on the matching between the measurement's influence and the interacting spectrum. Now, a question in point is whether measurements alone can induce decay. To answer this question, we study the case with far off-resonant couplings in this paper. In other words, the characteristic level spacing of the system lies far away from the energy band of the bath. If there were no measurements, the decay could be negligible. We will show that the QAZE indeed takes place on condition that the bath provides a channel for energy relaxation.

As demonstrated in Ref. [11], a diversity of novel features arise from the interaction between a two-level system and a continuum with photonic band gaps. Enlightened by this discovery, we consider the QAZE in a two-level system coupled to a bath with a narrow band. The total system is made up of an artificial atom and a coupled-resonator waveguide with a narrow energy band, which was introduced to investigate the coherent transport for single photon.[12−13] In this system, the level spacing of the artificial atom is feasibly adjusted within and beyond the energy band of the bath. And the coupled-resonator waveguide can be thought of as a structured bath with a nonlinear dispersion relation. When the atomic transition frequency is tuned beyond the energy band of the bath, the atomic decay is induced purely by the measurements in contrast to the originally suppressed one. What is more important, besides the bare excited state, our calculation also shows that the QAZE exists for the physical excited state. This situation is different from the case for the hydrogen atom where the QAZE does not occur for the physical excited state[14] but the bare excited state.[15] We emphasize that the reported phenomenon is a pure QAZE which is repressed if no measurement is applied to the artificial atom.

In our consideration, starting from a general Hamiltonian without the rotating-wave approximation (RWA),[16] we obtain an effective Hamiltonian by the generalized Fröhlich–Nakajima transformation and thus the effective decay rate modified by the measurements. In general cases, the effect of the counter-rotating terms can be omitted for it only leads to a small correction to the atomic level spacing. But in some special cases, i.e., near the edges of the bath's energy band, the considerations with

*Supported by the Natural Science Foundation of China under Grant Nos. 10974209 and 10935010 and by the National 973 Program under Grant No. 2006CB921205 and China Postdoctoral Science Foundation under Grant No. 20100470584

and without the RWA seem to result in the opposite predictions of the atomic decay. However, from an exact solution to the Schrödinger equation without the Wigner–Weisskopf approximation, we find out that there is no singular behavior in this case.

The paper is structured as follows. In the next section, we describe the total system including an artificial atom and a structured bath formed by a coupled-resonator waveguide. With a generalized Fröhlich–Nakajima transformation, we obtain the effective Hamiltonian and thus the decay rate. Moreover, we discuss the pure QAZE for both the bare excited state and the physical excited state in Sec. 3. Since there may be singular behavior for the decay phenomenon at the edges of the reservoir's energy band, we analyze this situation from the exact solution to the Schrödinger equation. Before a brief conclusion is summarized in Sec. 4, we present two proposals to put this model into practice in Sec. 5. Finally, in order to investigate the singular behavior of the golden rule decay rate near the band edge, we offer an exact solution to the Schrödinger equation without the Wigner–Weisskopf approximation in Appendix.

2 Model Description

We consider a structured bath described by the Hamiltonian

$$H_B = \sum_k \omega_k b_k^\dagger b_k \,, \tag{1}$$

where b_k and $b_k^\dagger$ are the annihilation and creation operators of the k-th mode, respectively. It possesses a nonlinear dispersion relation

$$\omega_k = \omega_0 - 2\zeta \cos k \,, \tag{2}$$

which forms an energy band centered at ω_0 with width 4ζ, as shown in Fig. 1. Therein, we offer two situations where the atomic level spacing is located beyond the energy band of the reservoir. To realize the above physical setup, we propose two artificial architectures in circuit QED and photonic crystal plus quantum dot, which will be shown explicitly in the Sec. 5.

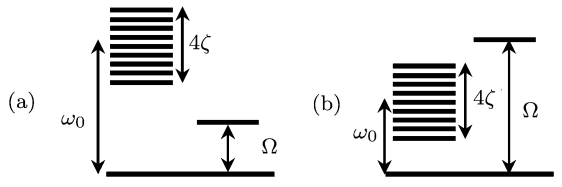

Fig. 1 The energy diagram of the total system. The level spacing of the system is Ω, while the energy spectrum of the bath is a band centered at ω_0 with width 4ζ. The level of the system's excited state lies (a) below the lower limit of the band or (b) above the upper limit of the band.

Besides, an artificial atom with level spacing Ω governed by the free Hamiltonian,

$$H_S = \frac{\Omega}{2}\sigma_z \,, \tag{3}$$

interacts with the structured bath. Here, $\sigma_z \equiv |e\rangle\langle e| - |g\rangle\langle g|$ is the Pauli operator with $|e\rangle$ and $|g\rangle$ being the atomic excited and ground states, respectively. The interaction Hamiltonian between the atom and the bath is given by

$$H_I = \sum_k g_k (b_k + b_k^\dagger)(\sigma^+ + \sigma^-) \,, \tag{4}$$

where $\sigma^+ = (\sigma^-)^\dagger \equiv |e\rangle\langle g|$ are the raising and lowering operators for the atom, and we introduce the coupling constants

$$g_k \equiv \frac{g}{\sqrt{N}} \,, \tag{5}$$

which are equal for the N modes. It should be emphasized that in the interaction Hamiltonian (4) we do not impose the RWA.

Thus, the total system including the atom and the bath is governed by the Hamiltonian

$$H = H_S + H_B + H_I \,. \tag{6}$$

Due to the insolvability of the original Hamiltonian (6), we follow the method introduced in Ref. [15], which is the generalized version[17] of the Fröhlich–Nakajima transformation,[18–19] to attain an effective Hamiltonian

$$\begin{aligned} H_{\rm eff} &\simeq e^{-S} H e^{S} \\ &\simeq H_0 + H_1 + \frac{1}{2}[H_1, S] + \frac{1}{2}[H_I, S] \,, \end{aligned} \tag{7}$$

where $H_1 = H_I + [H_0, S]$ is the first order term.

In order to eliminate the high-frequency terms $b_k^\dagger \sigma^+ +$ h.c., we choose the operator

$$S = \sum_k A_k (b_k^\dagger \sigma^+ - b_k \sigma^-) \,, \tag{8}$$

with

$$A_k = -\frac{g_k}{\omega_k + \Omega} \,. \tag{9}$$

Then we have

$$H_1 = \sum_k g_k (b_k \sigma^+ + \text{h.c.}) \,. \tag{10}$$

Further calculation shows that

$$[H_1, S] = -\sum_{k,k'} A_{k'} g_k (b_k^\dagger b_{k'}^\dagger + b_{k'} b_k)\sigma_z \,, \tag{11}$$

$$\begin{aligned} [H_I, S] = &-\sum_{k,k'} A_{k'} g_k [(b_k^\dagger b_{k'} + b_{k'}^\dagger b_k)\sigma_z - 2\sigma^-\sigma^+\delta_{kk'}] \\ &+ [H_1, S] \,. \end{aligned} \tag{12}$$

By omitting the high-frequency terms including $b_k^\dagger b_{k'}$ $(k \neq k')$ and $b_k^\dagger b_{k'}^\dagger + b_{k'} b_k$ in the above equations, we obtain

$$H_{\rm eff} = \sum_k \omega_k b_k^\dagger b_k + \frac{\Omega}{2}\sigma_z + \sum_k g_k (\sigma^+ b_k + \text{h.c.})$$

$$-\sum_k A_k g_k b_k^\dagger b_k \sigma_z + \sum_k A_k g_k \sigma^- \sigma^+ . \quad (13)$$

For the case of single excitation, the fourth term on the right hand side of Eq. (13) results in a small correction to the final consequence and thus can be dropped off. In all, the effective Hamiltonian is approximated as

$$H_{\text{eff}} = \sum_k \omega_k b_k^\dagger b_k + \frac{\Omega_1}{2}\sigma_z + \sum_k g_k(\sigma^+ b_k + \text{h.c.}) , \quad (14)$$

with the modified frequency

$$\Omega_1 = \Omega - \sum_k A_k g_k . \quad (15)$$

On account of the specific form of the interacting spectrum, the modified atomic level spacing defined in Eq. (15) is

$$\begin{aligned}\Omega_1 &= \Omega + \sum_k \frac{g_k^2}{\omega_k + \Omega} \\ &= \Omega + \frac{N}{2\pi}\int_{-\pi}^{\pi} \frac{g_k^2}{\omega_k + \Omega} dk \\ &= \Omega + \frac{g^2}{\sqrt{(\omega_0 + \Omega)^2 - 4\zeta^2}} . \end{aligned} \quad (16)$$

By comparing Eq. (14) with Eq. (6), we can see that the total effect of the counter-rotating terms is to alter the atomic level spacing while it leaves the couplings between the atom and the bath unchanged.

3 Pure Anti-Zeno Effect

When we come to the QAZE, we refer to the survival probability of the atomic excited state $|e\rangle$. In the previous studies,[15] for the bare excited state, we show that the QAZE still takes place in the presence of the countering-rotating terms. However, the QAZE is erased and only is the QZE left for the physical excited state.[14] In this section, we discover that the QAZE happens for both the two initial states in this artificial architecture.

3.1 *Quantum Anti-Zeno Effect for Spontaneous Decay*

In the following, we mainly focus on the QAZE for the spontaneous decay. In other words, the total system is initially prepared in the bare excited state $|e, \{0\}\rangle$, where the state $|\{0\}\rangle \equiv |0_1, \ldots, 0_k, \ldots 0_N\rangle$ denotes the vacuum for all of the bath's modes. Due to the specific transformation of the form as Eq. (8), the initial state after the transformation $\exp(-S)|e, \{0\}\rangle = |e, \{0\}\rangle$ is unaltered. The survival probability of the atomic excited state coincides with the one of the total system in its initial state,[15] i.e.,

$$\begin{aligned} P_e =& \text{Tr}_B(|e\rangle\langle e|e^{-iHt}|e, \{0\}\rangle\langle e, \{0\}|e^{iHt}) \\ \simeq& |\langle e, \{0\}|e^{-iH_{\text{eff}}t}|e, \{0\}\rangle|^2 . \end{aligned} \quad (17)$$

As shown in Ref. [15], for the present case the decay rate after repetitive measurements reads

$$R = 2\pi \int_{-\infty}^{\infty} d\omega F(\omega, \Omega_1, \tau) G(\omega) , \quad (18)$$

which is an overlap integration of the level broadening induced by measurements

$$F(\omega, \Omega_1, \tau) = \frac{\tau}{2\pi}\text{sinc}^2\left[\frac{(\omega - \Omega_1)\tau}{2}\right] , \quad (19)$$

and the interacting spectrum

$$G(\omega) = \sum\nolimits_k g_k^2 \delta(\omega - \omega_k) = g_k^2 \rho(\omega_k)|_{\omega_k = \omega} . \quad (20)$$

Also the interacting spectrum can be considered as the energy spectrum of the bath weighed by the atomic coupling constants. In the following discussions, we assume the resonator number N to be such a large number that it is reasonable to consider the density of state to be continuous in the frequency space. Here, the density of state in the coupled-resonator waveguide is

$$\begin{aligned}\rho(\omega_k) &= \frac{dn}{d\omega} = \frac{N}{2\pi}\left|\frac{dk}{d\omega_k}\right| = \frac{N}{2\pi}\left|\frac{1}{2\zeta \sin k}\right| \\ &= \frac{N}{\pi}\frac{1}{\sqrt{4\zeta^2 - (\omega_k - \omega_0)^2}} , \end{aligned} \quad (21)$$

where dn means the number of states within the frequency range $d\omega$. Note that in the second line of the above equation, we have used the fact that the distribution of the states in wavevector space is symmetric, with the density $N/(2\pi)$. According to Eqs. (2) and (21), we know that the density of state $\rho(\omega_k)$ has two singular points at both the ends of the band, as shown in Fig. 2.

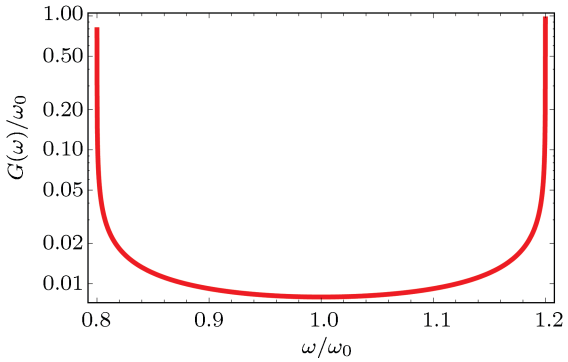

Fig. 2 (color online) The interacting spectrum $G(\omega)$ vs. ω with $\omega_0 = 1$, $g = 0.1$, and $\zeta = 0.1$. The interacting spectrum is centered at ω_0 $(= 1)$ and with width 4ζ $(= 0.4)$, i.e., extending from 0.8 to 1.2. There are two singular points ($\omega/\omega_0 = 0.8$ and 1.2) at the two ends of the energy band.

And we can numerically verify that it fulfills the requirement for normalization, i.e.,

$$\lim_{\xi \to 0} \int_{\omega_0 - 2\zeta + \xi}^{\omega_0 + 2\zeta - \xi} \rho(\omega) d\omega = N . \quad (22)$$

Substitution of Eq. (21) for $\rho(\omega_k)$ in Eq. (20) leads to

$$G(\omega) = \frac{g^2}{\pi}\frac{1}{\sqrt{4\zeta^2 - (\omega - \omega_0)^2}} . \quad (23)$$

Clearly, this interacting spectrum is nonzero within the energy band of the bath, ranging from $\omega_0 - 2\zeta$ to $\omega_0 + 2\zeta$, while beyond the energy band it vanishes. This property

of the interacting spectrum can help us to understand the appearance of the pure QAZE.

When we refer to the QAZE, we make a comparison between the instantaneous decay rate modified by the measurements and the unperturbed one, which is the so-called golden rule decay rate R_G. By and large, the latter can be obtained directly from the long time limit of Eq. (18), i.e., $R_{\rm G} = \lim_{\tau\to\infty} R$. In this case, since

$$\lim_{\tau\to\infty} F(\omega, \Omega_1, \tau) = \delta(\omega - \Omega_1)\,, \tag{24}$$

the golden rule decay rate

$$R_{\rm G} = 2\pi G(\Omega_1) \tag{25}$$

is determined by the interacting spectrum at the modified atomic level spacing.

Then, an interesting phenomena emerges. When there is no measurement applied to the atom and the modified atomic level spacing is located far beyond the energy band of the bath, it is obvious that the excited atom will not decay although it is coupled to the bath according to Eq. (25). It is a comprehensible result since there is no energy level of the bath in approximate resonance with the atomic transition frequency. In other words, there is no channel for the atomic excitation to relax. In this sense, the decay phenomenon is greatly suppressed and therefore we obtain a zero golden rule decay rate, i.e., $R_{\rm G} = 2\pi G(\Omega_1) = 0$. The same physical consequence could also be obtained from the Wigner–Weisskopf approximation.[20] On the other hand, when the atom is measured, we calculate the decay rate R according to Eq. (18) and find out that the decay phenomenon could be observed due to the repetitive measurements no matter how frequently the measurements are applied to atom. We remark that this is a pure QAZE as the measurement-induced decay rate is definitely larger than the vanishing golden rule decay rate. In Fig. 3, the measurement-induced decay rate is plotted for different measurement intervals. Therein, the level spacing of the atom is chosen as $\Omega = 2$, which is far beyond the bath's energy band ranging from 0.8 to 1.2. It is discovered that when we measure the atom repeatedly, the decay rate R is nonzero. It is totally different from the golden rule decay rate $R_{\rm G} = 0$ when there is no measurement applied to the atom. Therefore, the QAZE is purely induced by the measurements.

This pure QAZE can be physically explained as follows. When the atom evolves freely, there is only coupling between the atom and the bath. The excitation originally in the atom can not relax to the bath since its energy level is far beyond the bath's energy band and thus there are no modes of the bath in approximate resonance with the atomic transition frequency. However, as the measurements are applied, the inborn energy level is widely broadened.[8] As long as there is overlap between the atomic broadened level and the energy band of the bath, there exist channels for the atom to relax. Therefore, the decay phenomenon comes into being. Mathematically, the overlap integration (18) does not vanish in this case and thus results in a nonzero decay rate.

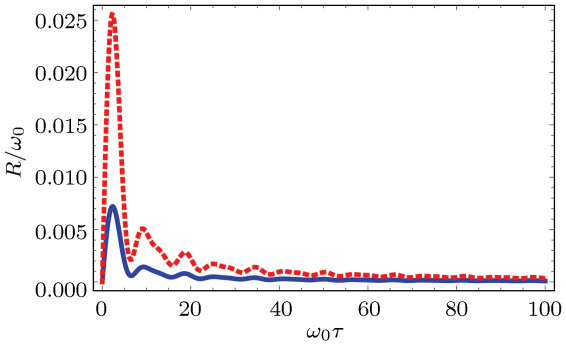

Fig. 3 (color online) The decay rate R versus the scaled time $\omega_0\tau$ with $\omega_0 = 1$, $\zeta = 0.1$, $g = 0.1$, and $\Omega = 2$. The solid line for the bare excited state while the dotted line for the physical excited state.

3.2 *Anti-Zeno Effect for Physical Excited State*

In the previous subsection, the QAZE is displayed for the total system initially prepared in the bare excited state $|e, \{0\}\rangle$. In Ref. [21], it was announced that the bare ground state should be replaced by the physical ground state $e^{S'}|g, \{0\}\rangle$ with the operator

$$S' = \sum_k A_k(b_k^\dagger\sigma^- - b_k\sigma^+ + b_k^\dagger\sigma^+ - b_k\sigma^-)\,, \tag{26}$$

due to the presence of the counter-rotating terms. Therefore, so far as the initial state is concerned, the physical excited state $e^{S'}|e, \{0\}\rangle$ substitutes for the bare excited state $|e, \{0\}\rangle$.[14] As a consequence, the QAZE disappears and only is the QZE present for the physical excited state.[14] In this subsection, we will show that the QAZE still exists for the physical excited state.

In this case, with respect to the physical excited state, the survival probability of the atomic excited state after a projective measurement is

$$\begin{aligned} P_e &= {\rm Tr}_B(|e\rangle\langle e|e^{-iHt}e^{S'}|e, \{0\}\rangle\langle e, \{0\}|e^{-S'}e^{iHt}) \\ &\simeq |\langle e, \{0\}|e^{-iH'_{\rm eff}t}|e, \{0\}\rangle|^2\,. \end{aligned} \tag{27}$$

As shown in the above equation, the survival probability with respect to the physical excited state under the original Hamiltonian (6) is equivalent to the one with respect to the bare excited state under an effective Hamiltonian

$$H'_{\rm eff} = \sum_k \omega_k b_k^\dagger b_k + \frac{\Omega'}{2}\sigma_z + \sum_k g'_k(\sigma^+ b_k + {\rm h.c.})\,, \tag{28}$$

with a modified level spacing

$$\Omega' = \Omega + 2\sum_k \frac{\Omega g_k A_k}{\omega_k + \Omega}\,, \tag{29}$$

and modified coupling constants

$$g'_k = \frac{2\Omega}{\omega_k + \Omega} g_k\,. \tag{30}$$

Straightforwardly, we obtain the corresponding decay rate after n repetitive measurements

$$R = 2\pi \int_{-\infty}^{\infty} d\omega F(\omega, \Omega', \tau) G'(\omega)\,, \tag{31}$$

which is an overlap integration of the level broadening induced by measurements centered at Ω'

$$F(\omega, \Omega', \tau) = \frac{\tau}{2\pi} \mathrm{sinc}^2\Big[\frac{(\omega - \Omega')\tau}{2}\Big]\,, \tag{32}$$

and the modified interacting spectrum

$$\begin{aligned} G'(\omega) &= \sum\nolimits_k (g_k')^2 \delta(\omega - \omega_k) \\ &= \frac{4\Omega^2}{(\omega_k + \Omega)^2} g_k^2 \rho(\omega_k)|_{\omega_k = \omega} \\ &= \frac{4g^2\Omega^2}{\pi(\omega + \Omega)^2 \sqrt{4\zeta^2 - (\omega - \omega_0)^2}}\,. \end{aligned} \tag{33}$$

Also in the long time limit, we obtain the corresponding golden rule decay rate

$$R_{\mathrm{G}} = 2\pi G'(\Omega')\,. \tag{34}$$

On condition that the modified level spacing is beyond the band, the golden rule decay rate vanishes similarly to the case with the bare excited state. Thus, if there were nonvanishing decay phenomenon due to the measurements, the pure QAZE would be observed. Yet, we plot the decay rate for this case in Fig. 3. Notice that the measurement-induced decay rate for the physical excited state is generally larger than the one for the bare excited state.

4 Decay Phenomenon Near Band Edge

As stated in the previous section, there are singular points at both the ends of the bath's energy band. On account of the discontinuous density of state at the edges of the band, we may justifiably anticipate some exceptional phenomena around the band edge, especially the ones due to the modification in the atomic level spacing. Generally speaking, the difference between the modified atomic level spacing and the original one is tiny small and thus can be neglected. However, for some special cases, it seems to lead to totally opposite predictions about the decay phenomenon induced by the coupling to the bath. We consider a specific case when the level spacing of the artificial atom is tuned to the neighborhood of the band edge, e.g., $\Omega < \omega_0 + 2\zeta$. If the distance between the original atomic level spacing and the band edge is so small that the modified level spacing is outside of the band. The theories with the RWA and without the RWA offer opposite predictions about the decay phenomenon, i.e., $R_{\mathrm{G}}^{\mathrm{RWA}} = 2\pi G(\Omega)$ is nonzero while $R_{\mathrm{G}} = 2\pi G(\Omega_1) = 0$ vanishes.

Besides, for the decay phenomenon exactly at the band edge, it seems that there would be no atomic excited state existing as the golden rule decay rate diverges due to the infinite large spectral density. Here, the occurrence of singularities in the density of state is closely related to the number of dimensions of the physical system.[22] Notwithstanding, all these controversies could be settled down if we resort to the exact solution to the Schrödinger equation, as shown in Appendix A.

The instantaneous decay rate without measurements is defined as

$$R(t) = -\frac{1}{|\alpha(t)|^2} \frac{d|\alpha(t)|^2}{dt}\,, \tag{35}$$

where the survival probability of the atomic excitation is

$$\begin{aligned} |\alpha(t)|^2 = \Big| A_1 e^{p_1 t} + A_2 e^{p_2 t} + \int_{-2\zeta}^{2\zeta} C(x) \\ \times \exp\Big[i\Big(\frac{\Omega_1}{2} - \omega_0 + x\Big)t\Big] dx \Big|^2\,, \end{aligned} \tag{36}$$

and its rate of change is

$$\begin{aligned} \frac{d|\alpha(t)|^2}{dt} =& 2\Re(I_1 \times I_2^*) \\ & - 2A_1 A_2 (ip_1 - ip_2) \sin(ip_1 - ip_2)t \\ & + 2\Re[(A_1 p_1 e^{p_1 t} + A_2 p_2 e^{p_2 t}) I_1^*] \\ & + 2\Re[(A_1 e^{p_1 t} + A_2 e^{p_2 t}) I_2^*]\,, \end{aligned} \tag{37}$$

where the integrals are defined as

$$I_1 = \int_{-2\zeta}^{2\zeta} C(x) \exp\Big[i\Big(\frac{\Omega_1}{2} - \omega_0 + x\Big)t\Big] dx\,, \tag{38}$$

$$\begin{aligned} I_2 = i \int_{-2\zeta}^{2\zeta} C(x) \Big(\frac{\Omega_1}{2} - \omega_0 + x\Big) \\ \times \exp\Big[i\Big(\frac{\Omega_1}{2} - \omega_0 + x\Big)t\Big] dx\,, \end{aligned} \tag{39}$$

with

$$C(x) = \frac{1}{\pi} \frac{g^2 \sqrt{4\zeta^2 - x^2}}{(4\zeta^2 - x^2)(\Omega_1 - \omega_0 + x)^2 + g^4}\,. \tag{40}$$

The sign $\Re(x)$ means the real part of x and the coefficients are given as

$$A_j = \frac{[(ip_j + \Omega_1/2 - \omega_0)^2 - 4\zeta^2]}{[(ip_j + \Omega_1/2 - \omega_0)^2 - 4\zeta^2] + (ip_j - \Omega_1/2)(ip_j + \Omega_1/2 - \omega_0)}\,. \tag{41}$$

And p_1 and p_2 are the two solutions to

$$\Big(ip - \frac{\Omega_1}{2}\Big)^2 \Big[\Big(ip + \frac{\Omega_1}{2} - \omega_0\Big)^2 - 4\zeta^2\Big] + g^4 = 0\,, \tag{42}$$

with

$$ip_1 + \frac{\Omega_1}{2} - \omega_0 > 2\zeta\,, \tag{43}$$

$$ip_2 + \frac{\Omega_1}{2} - \omega_0 < -2\zeta\,. \tag{44}$$

In order to show the above result explicitly, we plot the free evolution of the survival probability around the band edge in Fig. 4. It is seen that the initial atomic excitation will nonexceptionally decay into a steady value for the three cases, of which the atomic level spacings are distributed within the band, beyond the band and exactly at the band edge. Here, the original and modified atomic level spacing are tuned to the either side of the band edge. And the differences among the survival probabilities are negligible as the three frequencies are nearly identical.

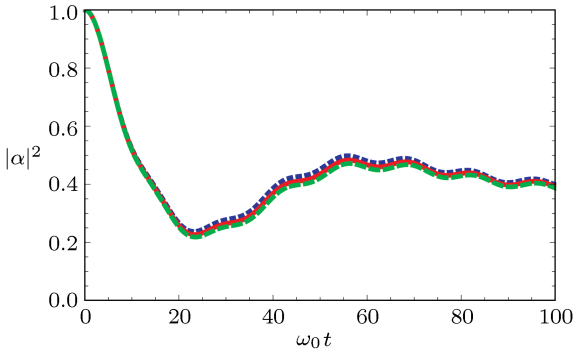

Fig. 4 (color online) The free evolution of the survival probabilities $|\alpha|^2$ near the band edge with $\omega_0 = 1$, $g = 0.1$, and $\zeta = 0.1$. The dotted line for the modified frequency $\Omega_1 = 1.203$ and the dashed line for the original frequency $\Omega = 1.198$. And the solid line is just the case with the atomic level spacing exactly at the band edge, i.e., $\Omega = 1.2$.

Besides, Fig. 5 presents the instantaneous decay rate for the above situations. It is seen that despite some oscillations around zero, the decay rate R always remains finite no matter whether the level spacing is at the band edge or not. And the differences between them is so small that we can neglect them. Further investigation shows the survival probability tends to be a steady value after an initial decay. Here, we emphasize that the divergent golden rule decay rate at the band edge is due to the improper Wigner–Weisskopf approximation made in the deduction. In this case, the spectral density varies sharply around the edge of the band. Since the atomic excitation decays into all of the channels around the atomic frequency, we shall average all the contributions from these channels instead of counting on the single one, which exactly equals the atomic frequency. Intuitionally, the decay rate for the atomic frequency at the band edge does not diverge.

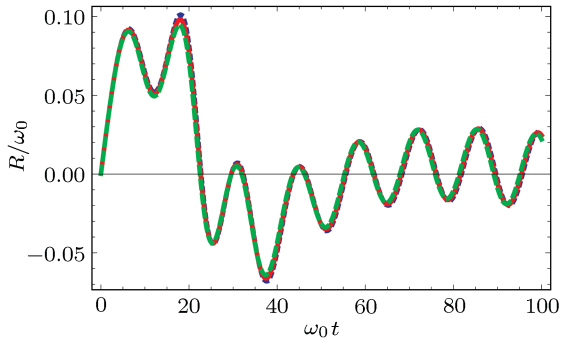

Fig. 5 (color online) The instantaneous decay rate R near the band edge with the same parameters given in Fig. 4. Notice that three curves are nearly overlap.

5 Physical Implementations of Artificial System

In this section, we propose two possible physical setups to observe the above phenomena. As mentioned above, the artificial system is composed of a tunable two-level system and a coupled-resonator waveguide. Therefore, the primal requirement for physical implementation is to provide a coupled-resonator array and a tunable two-level system, which is coherently coupled to one of the resonators in the waveguide. Currently, there are several potential candidates. For instance, in the superconducting circuit QED, a coupled superconducting transmission line resonator array can be realized to interact with a superconducting charge qubit. Besides, another potential candidate is the semiconductor microwave cavity QED, where coupled photonic crystal cavity array interacts with an artificial atom formed by a semiconductor quantum dot. In the following subsections we will address the two systems respectively.

5.1 *Circuit QED*

First of all, we consider the artificial system to be realized in the circuit QED[23] as shown in Fig. 6.

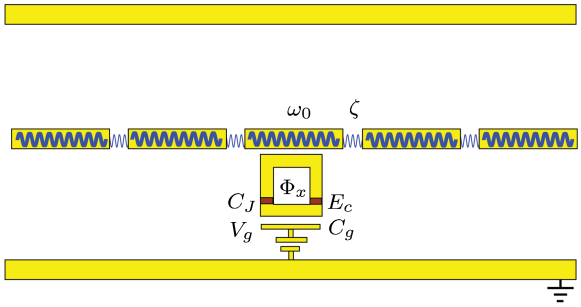

Fig. 6 (color online) Implementation in circuit QED. The total system consists of an artificial atom and a structured bath formed by a coupled transmission line resonator waveguide. The atom is a superconducting charge qubit, which is located at the zeroth resonator.

The artificial atom is a Cooper pair box, also called charge qubit, which is a dc current superconducting quantum interference device. It is a superconducting island

connected to two Josephson junctions. Around the degenerate point, the Cooper pair box is approximated as a two-level system with the level spacing

$$\Omega = \sqrt{B_x^2 + B_z^2}\,. \tag{45}$$

And the two eigen states are defined as

$$|g\rangle = \sin(\theta/2)|0\rangle + \cos(\theta/2)|1\rangle\,, \tag{46}$$

$$|e\rangle = \cos(\theta/2)|0\rangle - \sin(\theta/2)|1\rangle\,, \tag{47}$$

where $|0\rangle$ and $|1\rangle$ denote the states with 0 and 1 extra Cooper pair on the island, respectively. Here, we also introduce the mixing angle

$$\theta = \tan^{-1}\left(\frac{B_x}{B_z}\right). \tag{48}$$

On one hand, the level spacing Ω is tunable since the energy

$$B_x = 4E_c(2n_g - 1)\,, \tag{49}$$

which originates from the charging energy of

$$n_g = \frac{C_g V_g}{2e} \tag{50}$$

extra Cooper pair on the island, can be varied by changing the gate voltage V_g applied to the gate capacitor C_g. Here,

$$E_c = \frac{e^2}{2(C_g + 2C_J)}\,, \tag{51}$$

with C_J being the capacitance of the single Josephson junction. On the other hand, the level spacing can also be adjusted as the energy

$$B_z = 2E_J \cos\left(\frac{\pi\Phi_x}{\Phi_0}\right) \tag{52}$$

is induced by the controllable applied magnetic flux Φ_x, where E_J is the Josephson energy and Φ_0 is the flux quanta.

In addition, a coplanar transmission line resonator is cut into N pieces to form a coupled-resonator waveguide.[24] And the coupling constant ζ between two neighboring resonators is determined by the coupling mechanism. Placed at the antinode of single-mode electromagnetic field, the atom only interacts with the electric field with the coupling strength to be

$$g = \frac{eC_g \sin\theta}{C_g + 2C_J}\sqrt{\frac{\omega_0}{Lc}}\,, \tag{53}$$

where ω_0 is the frequency of the single mode in the transmission line with length L and capacitance per unit length c. For the experimentally accessible parameters, we have $\omega_0 \sim$ 5–10 GHz and $\Omega \sim$ 5–15 GHz.[25] Therefore, the above used parameters in Sec. 3 are realizable in practice.

5.2 *Photonic Crystal Plus Quantum Dot*

In addition to the circuit QED, the system can also be realized in the photonic crystal. As shown in Fig. 7, a two-dimensional photonic crystal is fabricated in a sandwich-like architecture. The crystal consists of a square lattice of high-index dielectric rods. We attain a defected cavity by removing three rods. And the coupled defected cavities form the artificial bath, while the quantum dot within the central layer plays the role as the artificial atom. The strong coupling between a quantum dot and a single cavity was experimentally realized.[26–28] Besides, multiple coupled photonic crystal cavities have been already achieved to show all-optical electromagnetically induced transparency.[29] And the model of coupled cavities in the photonic crystal was put forward to investigate theoretically photonic Feshbach resonance.[30]

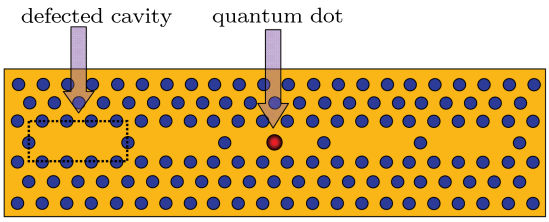

Fig. 7 (color online) Implementation in the photonic crystal. The system is made up of a photonic crystal cavity fabricated in a GaAs membrane containing a central layer with self-assembled InGaAs quantum dot inside. The quantum dot plays the part as an artificial atom.

6 Conclusion and Discussions

To summarize, we investigate the enhanced decay phenomenon in the total system composed of an artificial atom interacting with a structured bath. We apply a generalized Fröhlich–Nakajima transformation to obtain the effective Hamiltonian without the use of the RWA. It is discovered that the originally suppressed decay is enhanced due to the frequent projective measurements when the atomic frequency is tuned beyond the energy band of the reservoir. And the QAZE is present not only for the bare excited state but also for the physical excited state. This is different from the case for the hydrogen atom where the QAZE only exists for the former. We also remark that this is a pure QAZE entirely resulting from the measurement-induced atomic level broadening. Besides, we discuss the singular behavior of the golden rule decay rate near the band edge. Without the use of the Wigner–Weisskopf approximation, we attain the exact form of the unperturbed decay rate. It is found out that despite the oscillations the decay rate without measurements always remains finite in contrast to the divergent golden rule decay rate at the band edge. In addition, when the atomic frequency is tuned outside of the band, the exact decay rate tends to vanish in the long run, which is in accordance with the one obtained with the Wigner–Weisskopf approximation.

However, there are still some problems remaining. Generally speaking, the QAZE refers to the specific case where the measurement-induced decay rate is larger than

the unperturbed one, also called golden rule decay rate. In other cases, someone made a comparison between the decay phenomenon disturbed by the repetitive measurements and the free evolution, e.g., Ref. [31]. Besides, the interaction between the artificial bath and its environment broadens its energy band and thus the coupling spectrum. Therefore, the golden rule decay rate may not vanish due to the possible nonzero coupling spectrum at the atomic level spacing although it can be initially tuned outside of the bath's energy band. What is more important, the measurement used here is considered as an ideal projection. In some cases, by optically pumped into an auxiliary level, the population of the concerned level in the dynamical evolution was measured.[32] In the near future, we may study the QAZE for this case. Additionally, in this paper, we resort to the generalized Fröhlich–Nakajima transformation to solve the problem concerning the spontaneous decay disturbed by repetitive measurements without the RWA. When more complicated conditions are taken into consideration, this approach may not work due to the underlying difficulties, e.g., multiple excitations. We notice that a recent work[33] discussed various of situations such as different modulations and non-RWA aspects by means of projection operator techniques. This might be a possible method for problems under our consideration, e.g., the temperature's effect on the QAZE.

Appendix: Unperturbed Decay Rate without Wigner–Weisskopf Approximation

In this Appendix, we present an exact solution for the excited state population of an artificial atom interacting with a coupled-resonator waveguide. This problem is equivalent to the spontaneous emission of a two-level system interacting with a structured bath. Without the Wigner–Weisskopf approximation, we obtain the exact solution to the Schrödinger equation by the method of the Laplace transform.

The total system under our consideration is governed by the Hamiltonian

$$H=\sum_k \omega_k b_k^\dagger b_k+\frac{\Omega}{2}\sigma_z+\sum_k g_k(b_k\sigma^+ + b_k^\dagger\sigma^-)\,, \quad \text{(A1)}$$

where Ω_1 is replaced by Ω for ease of notation. Here the dispersion relation is

$$\omega_k=\omega_0-2\zeta\cos k\,, \quad \text{(A2)}$$

with $k\in(-\pi,\pi]$ and the coupling constants for all modes are equal as

$$g_k=\frac{g}{\sqrt{N}}\,. \quad \text{(A3)}$$

Since the total excitation number operator $\sum_k b_k^\dagger b_k+|e\rangle\langle e|$ of the system is a conservable quantity, we can express a general wavefunction, in single-excitation subspace, of the system at time t as

$$|\Psi(t)\rangle=\alpha(t)|e,\{0\}\rangle+\sum_k \beta_k(t)|g,1_k\rangle\,, \quad \text{(A4)}$$

where $|1_k\rangle\equiv|0_1,\ldots,1_k,\ldots 0_N\rangle$ denotes that the k-th mode possesses a single photon while other modes are in vacuum. By comparing the coefficients on the both sides of the Schrödinger equation

$$i\partial_t|\Psi(t)\rangle=H|\Psi(t)\rangle\,, \quad \text{(A5)}$$

we have

$$i\dot{\alpha}(t)=\frac{\Omega}{2}\alpha(t)+\sum_k g_k\beta_k(t)\,, \quad \text{(A6)}$$

$$i\dot{\beta}_k(t)=(\omega_k-\frac{\Omega}{2})\beta_k(t)+g_k\alpha(t)\,. \quad \text{(A7)}$$

By making the Laplace transform

$$\tilde{\alpha}(p)=\int_0^\infty dt\alpha(t)e^{-pt}\,, \quad \text{(A8)}$$

and by virtue of

$$\int_0^\infty dt\dot{\alpha}(t)e^{-pt}=p\tilde{\alpha}(p)-\alpha(0)\,, \quad \text{(A9)}$$

we obtain

$$\begin{aligned}\tilde{\alpha}(p)&=\frac{i\alpha(0)}{\Omega/2-ip+\sum_k g_k^2/[ip+(\Omega/2-\omega_k)]}\\&=\frac{1}{p+i(\Omega/2)+\sum_k g_k^2/[p+i(\omega_k-\Omega/2)]}\,,\end{aligned} \quad \text{(A10)}$$

where we have used the initial condition

$$\alpha(0)=1,\quad \beta_k(0)=0\,. \quad \text{(A11)}$$

When the atomic level spacing is far off-resonant with all bath's modes, e.g.,

$$\Omega\gg\omega_0+2\zeta\,, \quad \text{(A12)}$$

p in the third term of the denominator on the right hand side of Eq. (A10) can be approximated as $-i\Omega/2$, namely the Wigner–Weisskopf approximation. By means of the inverse Laplace transformation, we have a nonvanishing atomic excitation amplitude

$$\alpha(t)=\exp\Big[-i\Big(\frac{\Omega}{2}+\frac{g^2}{\sqrt{(\omega_0-\Omega)^2-4\zeta^2}}\Big)t\Big]\,. \quad \text{(A13)}$$

All the effect of the coupling to the bath does not reduce its magnitude but contributes an additional phase. This result is consistent with the one obtained from the Fermi golden rule.

In the following, we will show the exact solution of $\alpha(t)$ since the above used Wigner–Weisskopf approximation may fail for the cases that there are modes approximately in resonance with the atomic excited level. In order to calculate $\alpha(t)$, we need to apply the inverse Laplace transform to $\tilde{\alpha}(p)$. Therefore we shall find the branch cut and poles of $\tilde{\alpha}(p)$ at first. The branch cut is defined as

the line of which the limits on the two sides are different from each other, i.e.,

$$p \in [i(\Omega/2 - \omega_0 - 2\zeta), i(\Omega/2 - \omega_0 + 2\zeta)]\,. \tag{A14}$$

The poles can be found directly from the solutions to

$$p + i\frac{\Omega}{2} + \sum_k \frac{g_k^2}{p + i(\omega_k - \Omega/2)} = 0\,. \tag{A15}$$

The third term on the left hand side of the above equation can be expressed as

$$\begin{aligned}
&\sum_k \frac{g_k^2}{p + i(\omega_k - \Omega/2)} \\
&= \frac{N}{2\pi}\int_{-\pi}^{\pi} dk \frac{g_k^2}{p + i(\omega_k - \Omega/2)} \\
&= \frac{g^2}{2\pi}\int_{-\pi}^{\pi} dk \frac{1}{p - i(\Omega/2 - \omega_0 + 2\zeta\cos k)} \\
&= \frac{g^2}{2\pi\zeta}\oint_{|z|=1} \frac{dz}{iz}\frac{1}{[p - i(\Omega/2 - \omega_0)]/\zeta - i(z + 1/z)} \\
&= \frac{g^2}{2\pi\zeta}\oint_{|z|=1} \frac{dz}{z^2 + [(ip + \Omega/2 - \omega_0)/\zeta]z + 1} \\
&= \frac{g^2}{2\pi\zeta}\oint_{|z|=1} \frac{dz}{z^2 + Mz + 1}\,,
\end{aligned} \tag{A16}$$

with

$$M = \frac{ip + \Omega/2 - \omega_0}{\zeta}\,. \tag{A17}$$

Obviously, there are two solutions

$$z_\pm = \frac{-M \pm \sqrt{M^2 - 4}}{2}\,, \tag{A18}$$

to the equation

$$z^2 + Mz + 1 = 0\,. \tag{A19}$$

In the case of

$$M > 2\,, \tag{A20}$$

or equivalently

$$ip + \frac{\Omega}{2} - \omega_0 > 2\zeta\,, \tag{A21}$$

we have

$$0 > z_+ > -1\,, \tag{A22}$$

which is within the integration loop and

$$z_- < -1\,, \tag{A23}$$

which is outside of the integral loop. Therefore,

$$\begin{aligned}
&\sum_k \frac{g_k^2}{p + i(\omega_k - \Omega/2)} = \frac{g^2}{2\pi i\zeta}\oint_{|z|=1} \frac{dz}{z^2 + Mz + 1} \\
&= \frac{g^2}{2\pi\zeta} 2\pi i \lim_{z\to z_+} \frac{(z - z_+)}{(z - z_+)(z - z_-)} \\
&= \frac{ig^2}{\zeta(z_+ - z_-)} = \frac{ig^2}{\zeta\sqrt{M^2 - 4}} \\
&= \frac{ig^2}{\sqrt{(ip + \Omega/2 - \omega_0)^2 - 4\zeta^2}}\,.
\end{aligned} \tag{A24}$$

By substituting the above equation into Eq. (A15), we attain

$$ip - \frac{\Omega}{2} - \frac{g^2}{\sqrt{(ip + \Omega/2 - \omega_0)^2 - 4\zeta^2}} = if_1(p) = 0\,. \tag{A25}$$

Notice that the solution to the above equation is p_1 which should fulfill the requirement in Eq. (A21).

Similarly, when

$$M < -2\,, \tag{A26}$$

or equivalently

$$ip + \frac{\Omega}{2} - \omega_0 < -2\zeta\,, \tag{A27}$$

we have

$$0 < z_- < 1\,, \tag{A28}$$

within the integral loop while

$$z_+ > 1\,, \tag{A29}$$

outside of the integral loop. As a consequence,

$$\sum_k \frac{g_k^2}{p + i(\omega_k - \Omega/2)} = \frac{-ig^2}{\sqrt{(ip + \Omega/2 - \omega_0)^2 - 4\zeta^2}}\,. \tag{A30}$$

Therefore, we obtain the equation for the other singular point p_2, i.e.,

$$ip - \frac{\Omega}{2} + \frac{g^2}{\sqrt{(ip + \Omega/2 - \omega_0)^2 - 4\zeta^2}} = if_2(p) = 0\,, \tag{A31}$$

which should fulfill the requirement in Eq. (A27).

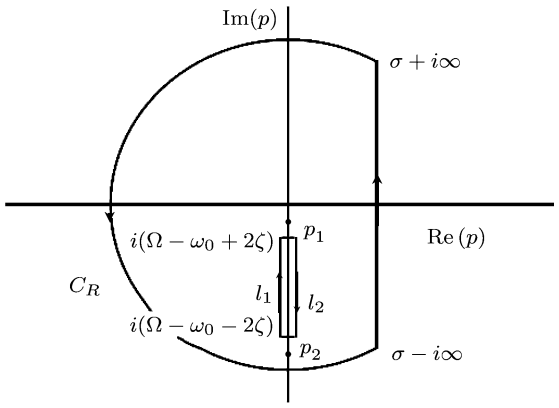

Fig. 8 Integration path for Eq. (A33).

In the following, we will calculate $\alpha(t)$ by making use of the inverse Laplace transform,

$$\alpha(t) = \frac{1}{2\pi i}\int_{\sigma-i\infty}^{\sigma+i\infty} dp\tilde{\alpha}(p)e^{pt}\,. \tag{A32}$$

As shown in Fig. 8, the contour integration is divided into four parts as follows

$$\int_{\sigma-i\infty}^{\sigma+i\infty} + \int_{C_R} + \int_{l_1} + \int_{l_2} = \oint = \sum_j \mathrm{res}[\tilde{\alpha}(p_j)e^{p_j t}]\,, \tag{A33}$$

where res$[F(p)]$ denotes the residue of function $F(p)$ at p. Thus, we have

$$\begin{aligned}\alpha(t) &= \frac{1}{2\pi i}\int_{\sigma-i\infty}^{\sigma+i\infty} dp\tilde{\alpha}(p)e^{pt} \\ &= \sum_j \text{res}[\tilde{\alpha}(p_j)e^{p_j t}] - \int_{C_R} - \int_{l_1} - \int_{l_2} \\ &= \sum_j \text{res}[\tilde{\alpha}(p_j)e^{p_j t}] - \int_{l_1} - \int_{l_2}, \end{aligned} \tag{A34}$$

where we have used the generalized Jordan Lemma[34]

$$\int_{C_R} = 0\,. \tag{A35}$$

For the pole determined by Eqs. (A21) and (A25), the residue is given as

$$\text{res}[\tilde{\alpha}(p_1)e^{p_1 t}] = \frac{e^{p_1 t}}{(df_1(p)/dp)|_{p=p_1}} = A_1 e^{p_1 t}\,, \tag{A36}$$

where

$$A_1 = \frac{[(ip_1+\Omega/2-\omega_0)^2-4\zeta^2]}{[(ip_1+\Omega/2-\omega_0)^2-4\zeta^2]+(ip_1-\Omega/2)(ip_1+\Omega/2-\omega_0)}\,. \tag{A37}$$

For the singular point given by Eq. (A31) and Eq. (A27), the residue is calculated as

$$\text{res}[\alpha(p_2)e^{p_2 t}] = \frac{e^{p_2 t}}{(df_2(p)/dp)|_{p=p_2}} = A_2 e^{p_2 t}\,, \tag{A38}$$

where

$$A_2 = \frac{[(ip_2+\Omega/2-\omega_0)^2-4\zeta^2]}{[(ip_2+\Omega/2-\omega_0)^2-4\zeta^2]+(ip_2-\Omega/2)(ip_2+\Omega/2-\omega_0)}\,. \tag{A39}$$

In the following we will calculate the contribution from the branch cut as

$$\begin{aligned} -\int_{l_1} - \int_{l_2} =& -\frac{1}{2\pi i}\Big[\int_{ip_{\min}}^{ip_{\max}} \frac{e^{pt}dp}{(p+i\Omega/2)+\sum\limits_k g_k^2/[p+i(\omega_k-\Omega/2)-0^+]} \\ &+\int_{ip_{\max}}^{ip_{\min}} \frac{e^{pt}dp}{(p+i\Omega/2)+\sum\limits_k g_k^2/[p-i(\Omega/2-\omega_k)+0^+]}\Big] \\ =& -\frac{1}{2\pi i}\Big[\int_{p_{\min}}^{p_{\max}} \frac{e^{ipt}dp}{(p+\Omega/2)-\sum\limits_k g_k^2/[p-(\Omega/2-\omega_k)+i0^+]} \\ &+\int_{p_{\max}}^{p_{\min}} \frac{e^{ipt}dp}{(p+\Omega/2)-\sum\limits_k g_k^2/[p-(\Omega/2-\omega_k)-i0^+]}\Big]\,, \end{aligned} \tag{A40}$$

where the limits for the integral are

$$p_{\min} = \Omega/2-\omega_0-2\zeta\,, \tag{A41}$$

$$p_{\max} = \Omega/2-\omega_0+2\zeta\,. \tag{A42}$$

In the denominator of Eq. (A40),

$$\begin{aligned} \sum_k \frac{g_k^2}{p-(\Omega/2-\omega_k)\pm i0^+} =& \frac{N}{2\pi}\int_{-\pi}^{\pi}\frac{g_k^2 dk}{p-(\Omega/2-\omega_k)\pm i0^+} = \frac{g^2}{2\pi}\int_{-\pi}^{\pi} dk\Big[\mathcal{P}\frac{1}{p-(\Omega/2-\omega_k)} \mp i\pi\delta\Big(p-\frac{\Omega}{2}+\omega_k\Big)\Big] \\ =& \frac{g^2}{2\pi}\Big[\int_{-\pi}^{\pi} dk\mathcal{P}\frac{1}{p-(\Omega/2-\omega_k)} \mp i2\pi\int_{\omega_0-2\zeta}^{\omega_0+2\zeta}\Big|\frac{dk}{d\omega_k}\Big|d\omega_k\delta\Big(p-\frac{\Omega}{2}+\omega_k\Big)\Big] \\ =& \frac{g^2}{2\pi}\Big[\int_{-\pi}^{\pi} dk\mathcal{P}\frac{1}{p-(\Omega/2-\omega_k)} \mp \int_{\omega_0-2\zeta}^{\omega_0+2\zeta}\frac{i2\pi}{2\zeta|\sin k|}d\omega_k\delta\Big(p-\frac{\Omega}{2}+\omega_k\Big)\Big] \\ =& \frac{g^2}{2\pi}\Big[\int_{-\pi}^{\pi} dk\mathcal{P}\frac{1}{p-(\Omega/2-\omega_k)} \mp \int_{\omega_0-2\zeta}^{\omega_0+2\zeta}\frac{i2\pi\delta(p-\Omega/2+\omega_k)}{\sqrt{(2\zeta)^2-(\omega_0-\omega_k)^2}}d\omega_k\Big] \\ =& \frac{g^2}{2\pi}\Big[\int_{-\pi}^{\pi} dk\mathcal{P}\frac{1}{p-(\Omega/2-\omega_k)} \mp \frac{i2\pi}{\sqrt{(2\zeta)^2-(\omega_0+p-\Omega/2)^2}}\Big]\,, \end{aligned} \tag{A43}$$

where the principal value function

$$\mathcal{P}\frac{1}{p-(\Omega/2-\omega_k)} = \begin{cases} 0, & \text{if } p-(\Omega/2-\omega_k)=0, \\ \dfrac{1}{p-(\Omega/2-\omega_k)}, & \text{if } p-(\Omega/2-\omega_k)\neq 0, \end{cases} \tag{A44}$$

and the additional factor 2 in the fourth line is due to the same contribution from $\pm k$.

And the first term on the right hand side of Eq. (A43)

$$\begin{aligned}
&\int_{-\pi}^{\pi} dk\mathcal{P}\frac{1}{p-(\Omega/2-\omega_k)}\\
&=\int_{-\pi}^{\pi} dk\mathcal{P}\frac{1}{p-\Omega/2+\omega_0-2\zeta\cos k}\\
&=\oint_{|z|=1}\frac{dz}{iz}\mathcal{P}\frac{1}{(p-\Omega/2+\omega_0)-\zeta(z+1/z)}\\
&=\oint_{|z|=1}\frac{dz}{-i\zeta}\mathcal{P}\frac{1}{z^2-(p-\Omega/2+\omega_0)z/\zeta+1}\\
&=\frac{2\pi i}{-i\zeta}\sum \mathrm{res}\Big[\frac{1}{z^2-(p-\Omega/2+\omega_0)z/\zeta+1}\Big]\,, \qquad \text{(A45)}
\end{aligned}$$

where the summation is over all the residues within the loop enclosed by $|z|=1$. Apparently, there are two solutions to the equation

$$z^2-\frac{p-\Omega/2+\omega_0}{\zeta}z+1=0\,, \qquad \text{(A46)}$$

i.e.,

$$z_\pm=\frac{M_1\pm i\sqrt{4-M_1^2}}{2}\,, \qquad \text{(A47)}$$

with

$$M_1=\frac{p-\Omega/2+\omega_0}{\zeta}\,. \qquad \text{(A48)}$$

For the branch cut

$$p\in[\Omega/2-\omega_0-2\zeta,\Omega/2-\omega_0+2\zeta]\,, \qquad \text{(A49)}$$

we have

$$M_1\in[-2,2]\,, \qquad \text{(A50)}$$

$$|z_\pm|=1\,. \qquad \text{(A51)}$$

Furthermore, due to the principal value function $\mathcal{P}$, the above two singular points are removed from the integral path. As a result,

$$\int_{-\pi}^{\pi} dk\mathcal{P}\frac{1}{p-(\Omega/2-\omega_k)}=0\,. \qquad \text{(A52)}$$

Then, by substituting the above equation into Eq. (A43), we have

$$\begin{aligned}
&\sum_k \frac{g_k^2}{p-(\Omega/2-\omega_k)\pm i0^+}\\
&=\mp\frac{ig^2}{\sqrt{(2\zeta)^2-(\omega_0+p-\Omega/2)^2}}\,. \qquad \text{(A53)}
\end{aligned}$$

Therefore, the contribution from the branch cut can be further simplified as

$$-\int_{l_1}-\int_{l_2}=\int_{-2\zeta}^{2\zeta}C(x)e^{i(\Omega/2-\omega_0+x)t}dx\,, \qquad \text{(A54)}$$

with

$$C(x)=\frac{1}{\pi}\frac{g^2\sqrt{4\zeta^2-x^2}}{(4\zeta^2-x^2)(\Omega-\omega_0+x)^2+g^4}\,. \qquad \text{(A55)}$$

In conclusion, the final solution is written as

$$\begin{aligned}
\alpha(t)&=\sum_j \mathrm{res}[\alpha(p_j)e^{p_jt}]-\int_{l_1}-\int_{l_2}\\
&=A_1e^{p_1t}+A_2e^{p_2t}\\
&\quad+\int_{-2\zeta}^{2\zeta}C(x)e^{i(\Omega/2-\omega_0+x)t}dx\,, \qquad \text{(A56)}
\end{aligned}$$

where the coefficients A_1, A_2, and $C(x)$ are real as given in Eqs. (A37), (A39), and (A55) respectively. Here, two pure imaginary numbers p_j are the solutions to

$$(ip-\Omega/2)^2[(ip+\Omega/2-\omega_0)^2-4\zeta^2]+g^4=0\,, \qquad \text{(A57)}$$

with

$$ip_1+\Omega/2-\omega_0>2\zeta\,, \qquad \text{(A58)}$$

$$ip_2+\Omega/2-\omega_0<-2\zeta\,. \qquad \text{(A59)}$$

The decay rate without measurement is defined as

$$R(t)=-\frac{d|\alpha(t)|^2}{dt}\Big/|\alpha(t)|^2\,, \qquad \text{(A60)}$$

where the survival probability for the initial state is

$$\begin{aligned}
|\alpha(t)|^2=&\Big|A_1e^{p_1t}+A_2e^{p_2t}\\
&+\int_{-2\zeta}^{2\zeta}C(x)e^{i(\Omega/2-\omega_0+x)t}dx\Big|^2\,, \qquad \text{(A61)}
\end{aligned}$$

and its rate of change is

$$\begin{aligned}
\frac{d|\alpha(t)|^2}{dt}&=2\Re(I_1\times I_2^*)\\
&\quad-2A_1A_2(ip_1-ip_2)\sin(ip_1-ip_2)t\\
&\quad+2\Re[(A_1p_1e^{p_1t}+A_2p_2e^{p_2t})I_1^*]\\
&\quad+2\Re[(A_1e^{p_1t}+A_2e^{p_2t})I_2^*]\,, \qquad \text{(A62)}
\end{aligned}$$

where the integrals are defined as

$$I_1=\int_{-2\zeta}^{2\zeta}C(x)e^{i(\Omega/2-\omega_0+x)t}dx\,, \qquad \text{(A63)}$$

$$I_2=\int_{-2\zeta}^{2\zeta}C(x)e^{i(\Omega/2-\omega_0+x)t}i\Big(\frac{\Omega}{2}-\omega_0+x\Big)dx\,, \qquad \text{(A64)}$$

and $\Re(x)$ is the real part of x.

Acknowledgement

We would like to express our gratitude towards T. Shi and Y. Li for many stimulating discussions. One of the authors (A.Q.) thanks G. Gordon for his valuable comments on the manuscript.

References

[1] H.P. Breuer and F. Petruccione, *The Theory of Open Quantum Systems*, Oxford University Press, Oxford, New York (2002).

[2] L.H. Yu and C.P. Sun, Phys. Rev. A **49** (1994) 592.

[3] C.P. Sun and L.H. Yu, Phys. Rev. A **51** (1995) 1845.

[4] L.S. Khalhin, JETP Lett. **8** (1968) 65.
[5] B. Misra and E.C.G. Sudarshan, J. Math. Phys. (N.Y.) **18** (1977) 756.
[6] K. Koshinoa and A. Shimizu, Phys. Rep. **412** (2005) 191.
[7] A.G. Kofman and G. Kurizki, Phys. Rev. A **54** (1996) R3750.
[8] A.G. Kofman and G. Kurizki, Nature (London) **405** (2000) 546.
[9] M.C. Fischer, B. Gutiérrez-Medina, and M.G. Raizen, Phys. Rev. Lett. **87** (2001) 040402.
[10] N. Bar-Gill, E.E. Rowen, G. Kurizki, and N. Davidson, Phys. Rev. Lett. **102** (2009) 110401.
[11] A.G. Kofman, G. Kurizki, and B. Sherman, J. Mod. Opt. **41** (1994) 353.
[12] L. Zhou, Z.R. Gong, Y.X. Liu, C.P. Sun, and F. Nori, Phys. Rev. Lett. **101** (2008) 100501.
[13] L. Zhou, S. Yang, Y.X. Liu, C.P. Sun, and F. Nori, Phys. Rev. A **80** (2009) 062109.
[14] H. Zheng, S.Y. Zhu, and M.S. Zubairy, Phys. Rev. Lett. **101** (2008) 200404.
[15] Q. Ai, Y. Li, H. Zheng, and C.P. Sun, Phys. Rev. A **81** (2010) 042116.
[16] M.O. Scully and M.S. Zubairy, *Quantum Optics*, Cambridge University Press, Cambridge, England (1997).
[17] H.B. Zhu and C.P. Sun, Science in China (A) **30** (2000) 928; Progeresses in Natural Sciences **10** (2000) 698.
[18] H. Fröhlich, Phys. Rev. **79** (1950) 845; Proc. Roy. Soc. A **215** (1952) 291; Adv. Phys. **3** (1954) 325.
[19] S. Nakajima, Adv. Phys. **4** (1953) 363.
[20] C.P. Sun, Y.D. Wang, Y. Li, and P. Zhang, in *Recent Progress in Quantum Mechanics,* Vol. III, edited by J.Y. Zeng, G.L. Long, and S.Y. Pei, Tsinghua University Press, Beijing (2003) p. 139.
[21] R. Loudon and S.M. Barnett, J. Phys. B: At. Mol. Opt. Phys. **39** (2006) S555.
[22] L.V. Hove, Phys. Rev. **89** (1953) 1189.
[23] A. Blais, R.S. Huang, A. Wallraff, S.M. Girvin, and R.J. Schoelkopf, Phys. Rev. A **69** (2004) 062320.
[24] J.Q. Liao, J.F. Huang, Y.X. Liu, L.M. Kuang, and C.P. Sun, Phys. Rev. A **80** (2009) 014301; J.Q. Liao, Z.R. Gong, L. Zhou, Y.X. Liu, C.P. Sun, and F. Nori, Phys. Rev. A **81** (2010) 042304.
[25] A. Wallraff, D.I. Schuster, A. Blais, L. Frunzio, R.S. Huang, J. Majer, S. Kumar, S.M. Girvin, and R.J. Schoelkopf, Nature (London) **431** (2004) 162.
[26] Y. Akahane, T. Asano, B.S. Song, and S. Noda, Nature (London) **425** (2003) 944.
[27] T. Yoshie, A. Scherer, J. Hendrickson, G. Khitrova, H.M. Gibbs, G. Rupper, C. Ell, O.B. Shchekin, and D.G. Deppe, Nature (London) **432** (2004) 200.
[28] D. Englund, A. Majumdar, A.F.M. Toishi, N. Stoltz, P. Petroff, and J. Vučković, Phys. Rev. Lett. **104** (2010) 073904.
[29] X.D. Yang, M.B Yu, D.L. Kwong, and C.W. Wong, Phys. Rev. Lett. **102** (2009) 173902.
[30] D.Z. Xu, H. Ian, T. Shi, H. Dong, and C.P. Sun, Sci. Chi Ser. G **53** (2010) 1234.
[31] I. Lizuain, J. Casabiva, J.J. Carcía-Ripoll, J.G. Muga, and E. Solano, arXiv:0912.3485 (2009).
[32] W.M. Itano, D.J. Heinzen, J.J. Bollinger, and D.J. Wineland, Phys. Rev. A **41** (1990) 2295.
[33] G. Gordon, J. Phys. B: At. Mol. Opt. Phys. **42**, (2009) 223001.
[34] K.M. Liang, *Method of Mathematical Physics*, Higher Education Press, Beijing (1998).